Bettahar, Houari; Freitas Vieira, Arthur; Zhou, Quan

Robotic Gel Dispensing based on Visual Servoing for Fiber Threading

Published in:
Proceedings - 2023 IEEE 47th Annual Computers, Software, and Applications Conference, COMPSAC 2023

DOI:
10.1109/COMPSAC57700.2023.00012

Published: 02/08/2023

Document Version
Peer-reviewed accepted author manuscript, also known as Final accepted manuscript or Post-print

Please cite the original version:
Bettahar, H., Freitas Vieira, A., & Zhou, Q. (2023). Robotic Gel Dispensing based on Visual Servoing for Fiber Threading. In H. Shahriar, Y. Teranishi, A. Cuzzocrea, M. Sharmin, D. Towey, AKM. J. A. Majumder, H. Kashiwazaki, J.-J. Yang, M. Takemoto, N. Sakib, R. Banno, & S. I. Ahamed (Eds.), *Proceedings - 2023 IEEE 47th Annual Computers, Software, and Applications Conference, COMPSAC 2023* (pp. 9-17). Article 10196880 (Proceedings : International Computer Software & Applications Conference). IEEE. https://doi.org/10.1109/COMPSAC57700.2023.00012

Robotic Gel Dispensing based on Visual Servoing for Fiber Threading

Houari Bettahar, Member IEEE
Department of Electrical Engineering and Automation, School of Electrical Engineering, Aalto University, Espoo, Finland.
houari.bettahar@aalto.fi.

Vieira Arthur
Department of Electrical Engineering and Automation, School of Electrical Engineering, Aalto University, Espoo, Finland.
arthur.vieira@aalto.fi.

Quan Zhou, Member IEEE
Department of Electrical Engineering and Automation, School of Electrical Engineering, Aalto University, Espoo, Finland.
quan.zhou@aalto.fi

***Abstract*— Dispensing sessile droplets accurately on the top of the needle tip is important for applications such as fiber threading. In this paper, we propose an accurate online gel dispensing method to accurately dispense sessile droplets on top of the dispenser tip for highly repeatable fiber threading. We design a robotic gel dispenser based on positive-displacement piston dispensing that can accurately dispense sessile gel droplets of desired volume using visual servoing and adaptive model predictive control. An online gel volume estimation algorithm based on image processing is constructed to provide the estimation of the volume of the extruded gel droplet to the controller. To compensate for the nonlinear and time-varying process properties, the Adaptive Model Predictive Controller (MPC) adjusts its prediction model at runtime while satisfying a set of constraints. We employ the fiber threading technique based on impedance control with force tracking we developed recently to carry out the fiber threading experiments. To examine the benefits of the accurately dispensed droplet, multiple fibers threading experiments are conducted, where the repeatability of the fibers fabricated using the proposed methods are compared with two other methods: a) conventionally velocity regulation-based fiber fabrication, where the pulling force profile is not controlled, and b) fiber threading using impedance control with force tracking using a commercial time-pressure dispenser. The experimental results show that fibers fabricated using the proposed method have the highest repeatability based on the coefficient of variation of properties of the fabricated fibers, where the obtained coefficient of variation of the toughness, stiffness, elongation, and strength are 6.7%, 3.7%, 3.4%, 5.6% respectively.**

***Index Terms*— micromanipulation, artificial fiber threading, bio-mimicking, visual servoing.**

I. INTRODUCTION

Various functional 3D objects require materials with fiber-like morphology, which can offer enhanced mechanical and physical properties. For example, hydrogel microfiber structures have been used to recapitulate the architecture and functionality of biological tissues at the microscale [1], [2]. Fibers have also been used fabricate actuators and sensors with at macro- and microrobotics [3]–[6].

A variety of techniques have been employed, e.g., wet-spinning [7], dry-spinning [8], electrospinning [9], microfluidic spinning [10], and direct writing [11]. So far, the strength and toughness of the produced artificial fibers can reach only about one-fifth of that of natural fibers such as spider silk fiber [12]. One of the reasons is that the fabrication process is either manual or based on open-loop regulation, e.g., velocity or position regulation. Many natural species, on the other hand, such as spiders [13] and silkworms [14] can conduct sophisticated pultrusion that can tune the mechanical properties of the fibers during threading by changing the pulling forces. This allows the gel protein (dope) to be continuously converted into fibers with exceptional mechanical properties [12].

To replicate the pultrusion mechanism, it was introduced in work [15] [16] a robotic gel fiber threading method based on impedance control with force tracking. The robotic threading method produced fibers with better mechanical properties compared with fibers fabricated using traditional open-loop velocity regulation. However, the initial volume of the gel droplet was not well controlled, impairing the repeatability of the mechanical properties of the fabricated fiber.

On the other hand, the problem of volume precision has been tackled in other liquid dispensing applications using many dispensing methods, e.g., piston dispensers [17], time-pressure dispensers [18], jet dispensers [19], and screw dispensers [20]. Different modeling and control approaches have also been investigated. For example, offline control schemes have been proposed, where the control action is based on the Bang-Bang controller [21] or incremental compensator [22]. Online control methods have also been proposed, commonly achieved using feedback control based on a proportional (P) or proportional-integral (PI) controller, where volume estimation is achieved based on modeling[23]–[25], or computer vision [26]. However, in these works, the droplets are first formed as a pendant and then placed on a target surface. There is no literature reporting dispensing a sessile droplet where the drop remains attached to the dispenser needle tip during threading [16] [15].

It is very challenging to dispense such a sessile droplet with precise volume since the non-Newtonian and time-varying properties of the fluid during dispensing makes the relationship between the piston displacement and volume non-linear. Additionally, overflowing could be catastrophic where the dispensing process cannot be recovered without cleaning the dispensing needle and workspace.

In this paper, we propose an accurate online gel dispensing method to dispense sessile droplets on the top of the dispenser tip for highly repeatable fiber threading. We design a robotic gel

*Research supported by Academy of Finland Project 317018.

dispenser based on positive-displacement piston dispensing that can accurately dispense sessile gel droplets of desired volume using visual servoing and adaptive model predictive control. An online gel volume estimation algorithm based on image processing is constructed to provide the estimation of the volume of the extruded gel droplet to the controller. To compensate for the nonlinear and time-varying process properties, an adaptive MPC adjusts its prediction model at runtime while satisfying a set of constraints. Fiber threading technique based on impedance control with force tracking developed recently [15], has been used to carry out the fiber threading experiments, where the whole approach is abbreviated as IMPVC in short. To examine the benefits of the precisely dispensed droplet, multiple fiber threading experiments are conducted, where the repeatability of the fibers fabricated using the proposed IMPVC is studied and compared with two other methods: a) conventionally velocity regulation-based fiber threading, where the pulling force is not controlled, referred to as VRVC method; and b) fiber threading using impedance control with force tracking introduced, where a commercial dispenser is used instead of the dispensing method proposed in this paper, referred to as IMPCD method.

The paper is organized as follows. Section II formulates the problem. Section III describes the experimental setup. Section IV introduces the estimation method for the extruded gel volume. Section V discusses the adaptative MPC approach for gel dispensing control. Section VI reports and discusses the experimental results. Finally, section VII concludes the paper.

II. Problem Formulation

Dispensing a sessile droplet on the top of the needle tip is important for studying the fiber threading [15], where the droplet will remain at its location during threading (see Fig. 1). Accurate droplet dispensing is one of the most crucial steps for acquiring reliable and repeatable results with respect to toughness, strength, elongation, and stiffness. The fiber threading experimental protocol is shown in **Fig.1 (A),** consisting of the fabrication and characterization phase. In the fabrication phase, a sessile gel droplet is firstly dispensed on the top of the tip of the dispenser needle; then the tip with the droplet approaches and contacts the tip of the force sensor; after that, the dispenser moves away from the force sensor pulling the gel droplet into a fiber using impendence control with force tracking [15], until certain reference force is satisfied; the system then stalls for a certain period to allow the fiber to solidify under solidification force control. In the characterization phase, the fiber is pulled further until the fiber breaks while the pulling force is recorded. This phase results in force-extension curves similar to **Fig. 1 (B)**.

The force-extension curves can reveal key mechanical properties of fiber, e.g., toughness, stiffness, elongation, and strength. Toughness is the most remarkable property of biological materials. A material can consume energy and gets deformed without breaking up. The stiffness of the material affects the degree it deflects under a load, and the strength is the property of a material that opposes the deformation or breakdown of material in the presence of load forces. The elongation-to-break is the deformation of a sample when it breaks.

We studied the repeatability of the mechanical properties based on the fabrication protocol mentioned above, whereas a

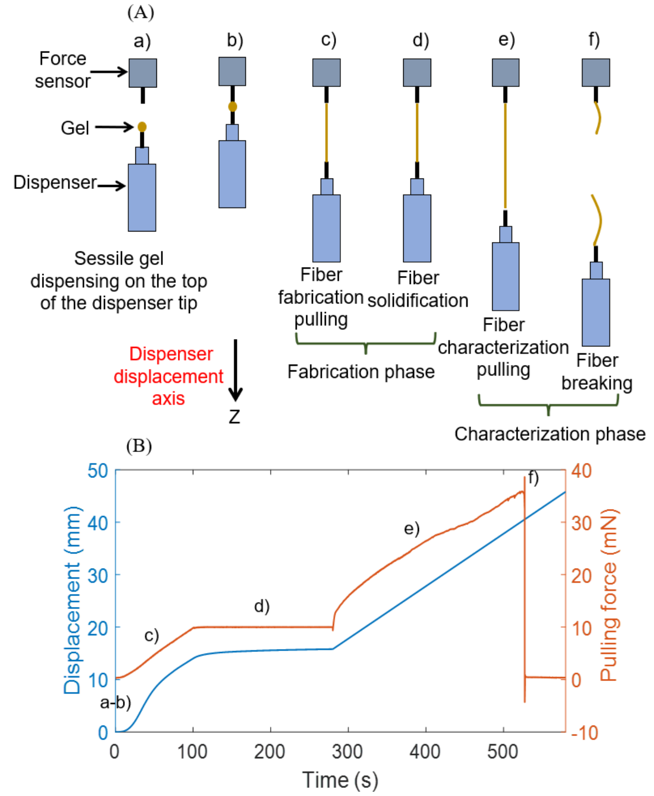

Fig. 1. (A) The fiber threading experimental protocol. a) a droplet of gel is extruded at the tip of the dispenser needle; b) the dispenser approaches and contacts the tip of the force sensor; c) the dispenser moves away from the force sensor pulling the gel droplet into a fiber using impendence control with force tracking until certain reference force is satisfied; d) the system stalls for a certain period to allow the fiber to solidify under solidification force control; e) the fiber is pulled further until f) the fiber breaks. (B) shows the force and displacement curves during the process steps a)-f).

commercial dispenser (Nordson EFD, model Performus V) is used, by setting the same dispensing parameters (pressure of 2 bars and dispensing time of 10 s). The obtained characterization force-extension curves are shown in **Fig. 2** and the mean, standard deviation (SD), and coefficient of variation (CV) of the mechanical properties are shown in Table 1.

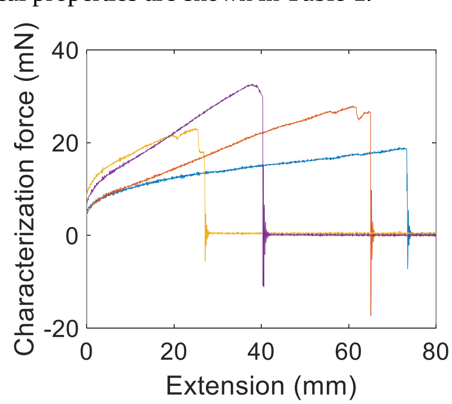

Fig.2. Force-extension curves during characterization based on IMPCD.

TABLE 1: TOUGHNESS, STIFFNESS, ELONGATION, AND STRENGTH, FOR FIBER FABRICATED BASED ON IMPCD

	Toughness ($MJ \cdot m^{-3}$)	Stiffness (N/m)	Elongation (%)	Strength (MPa)
Mean	1.02	0.36	519.5	25.60
SD	0.43	0.20	21.50	5.95
CV (%)	42.16	55.56	8.48	23.24

We attribute the low repeatability of the toughness, stiffness, and strength, elongation to the poor volume consistency even though the dispenser parameters are the same, where the mean and SD of the dispensed volume for 30 repetitions are 0.53 and 0.19 mm^3, respectively. We hypothesize that the initial volume has a significant impact on the mechanical properties of the fabricated fibers. For this reason, we propose a precise robotic gel dispensing method based on visual servoing using adaptative MPC.

III. EXPERIMENTAL SETUP

The experimental setup for fiber threading is shown in **Fig.3**. A novel precise robotic gel dispenser is installed at the lower part of the setup, mounted on a motorized precision positioner (Physik Instrumente, model M-404.4PD). A first surface mirror is placed behind the tip of the dispenser at an angle of 45° to provide two orthogonal views of the droplet for vision-based volume estimation. For pulling experiments, a needle is mounted on a fixed force sensor (LCM Systems, model LCM UF1) to sense the pulling force after contacting the gel at the tip of the gel dispenser. The motorized precision positioner is controlled via a controller (Physik Instrumente, model C-884.4CD). The measurement of the force sensor is acquired using a data acquisition (DAQ) board (National Instrument, model PCIe-6363). The whole setup is constructed on a vibration isolation table.

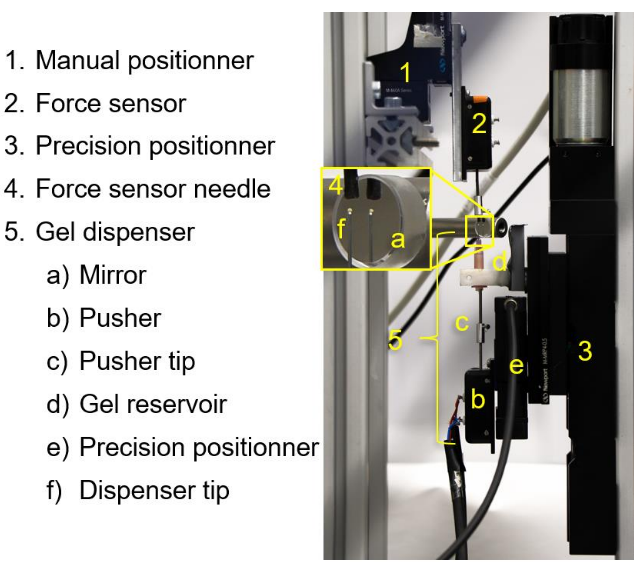

Fig. 3. The experimental setup for precision extrusion and robotic fiber micromanipulation and threading. The force sensor is fixed on a frame, and the gel dispenser is mounted on a motorized precision stage.

The dispenser consists of both mobile and fixed parts. The mobile part consists of a pusher with a tip. The pusher is fixed on a motorized precision positioner (Physik Instrumente, model M-122.2DD), controlled via a controller (Physik Instrumente, model C-884.4CD). The fixed part consists of a dispensing head, which includes a gel reservoir and a needle tip for gel dispensing. The gel reservoir is enclosed by a piston, which can slide inside the reservoir when pushed by the pusher tip, causing the dispenser extrudes the gel. The whole experimental setup including the dispenser is controlled using Matlab/Simulink. A commercial fast-curing contact adhesive (Pattex), a solvent-based polychloroprene rubber, is used as the gel specimen in the experiments.

IV. ONLINE GEL VOLUME ESTIMATION

The dispensed gel volume from the dispenser is one of the important parameters that can influence the mechanical properties of the fabricated fibers. To control the volume of the extruded gel, we propose an online vision-based estimation algorithm.

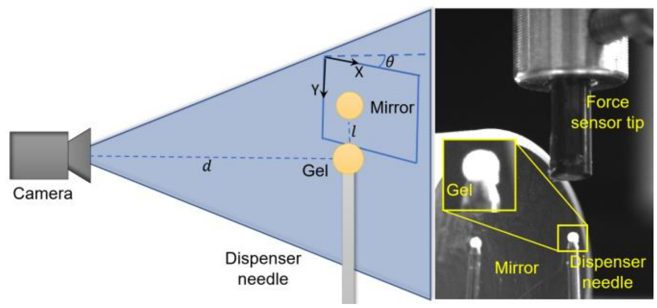

Fig. 4. Concept and experimental setup of the gel volume estimation method using two views.

To estimate the volume with good accuracy, we observe the shape of the droplet from two angles to account for the non-axial symmetric shape of the droplet, which is different from the traditional assumption that the droplet is rotationally symmetric and the volume of the droplet can be estimated using a single two-dimensional droplet contour [27], [26]. A mirror is placed behind the end of the dispenser tip at an angle of $\theta = 45°$ to provide a side view of the extruded droplet. The distance between the mirror and the dispenser tip is $l = 7$ mm on the axis passing by the end of the dispenser tip perpendicular to the axis between the center of the camera and the dispenser tip. A camera is placed at a distance $d = 82\ mm$ from the end of the tip of the dispenser as shown in **Fig.4**. This configuration allows acquiring two views, the front view and the side view reflected by the mirror. Images acquired from the two views are firstly converted to binary images using thresholding. Then, the largest connected object (the gel droplet) is extracted together with its exterior boundaries (see **Fig. 5 (a)**).

To achieve online 3-dimensional volume estimation, a facile volume estimation algorithm is developed using the two exterior boundaries (contours) of the gel droplet. The first step is to match the points in the first contour to the second one on the horizontal lines, where the spaces enclosed by the contours are segmented

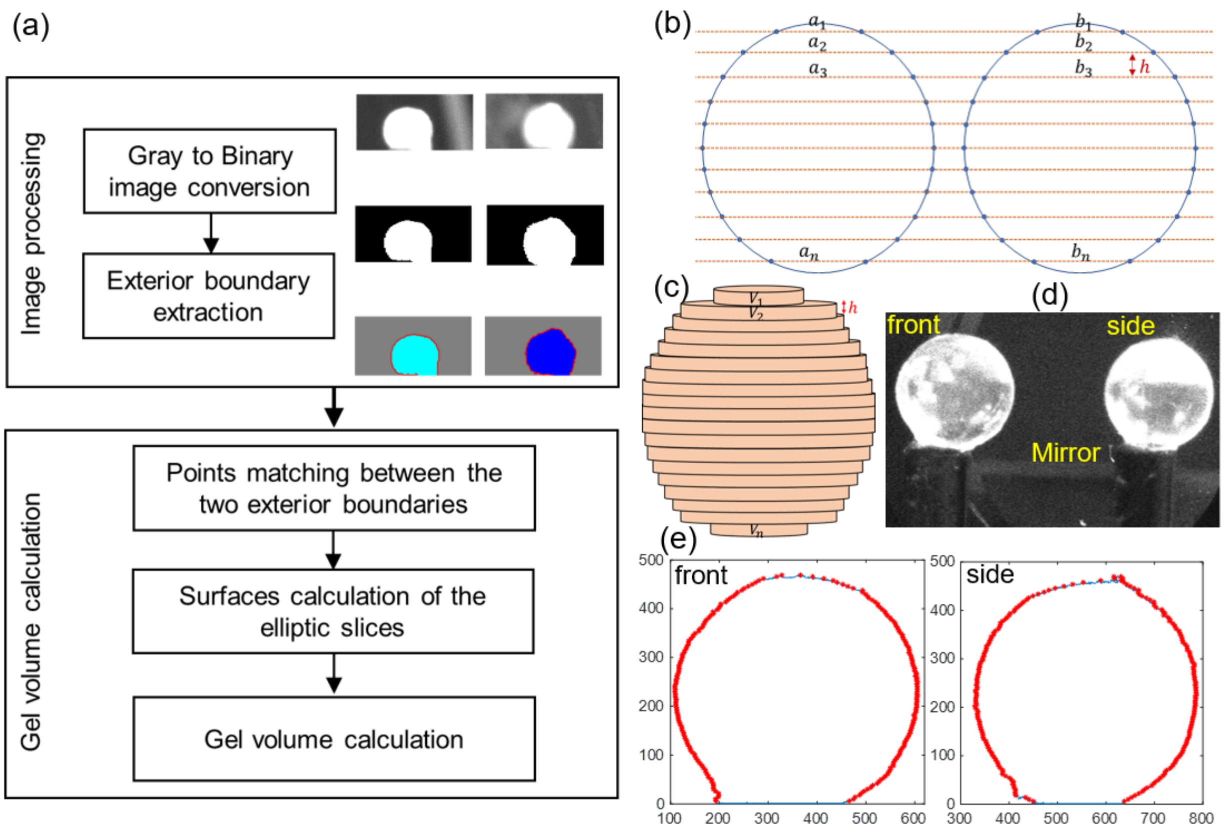

Fig. 5. (a) Algorithm for gel volume estimation. (b) The matching of the points in the first contour with respect to the second contour for the two image views. (c) The principle by which the droplet volume is estimated. (d) The front and side views of a sphere with known volume for the calibration of the algorithm. (e) The matching points in the first contour (front view) with respect to the second contour (side view) of the calibration sphere.

vertically in n slices of height h as shown in **Fig. 5 (b)**. Since the gel droplet is generally round, we treat each slice as an ellipse. The second step is then to take the four intersection points of each segment of the two contours to construct a two-dimensional ellipse. The third step is to calculate each elliptical disk volume using the equation: $V_i = \frac{\pi h}{4} a_i b_i$. By summing up all the n elliptical disks (see **Fig.5 (c)**), the volume of the droplet can be estimated:

$$V = \sum_{i=1}^{n} V_i = \frac{\pi h}{4} \sum_{i=1}^{n} a_i b_i \qquad (1)$$

where a_i and b_i are the lengths of the semi-major and semi-minor axes of the ith elliptical disk, respectively.

To validate the estimation algorithm, a ruby ball of known volume (diameter = 3.00 mm, volume = 14.1372 mm^3) is used as the specimen. The image of the actual sphere and its reflection in the mirror is shown in **Fig. 5 (d)**. The matching points of the two exterior boundaries derived using the slicing method are shown in **Fig. 5 (e)**. The estimation time of the volume is 0.02 seconds. The volume estimation algorithm was repeated 50 times. The obtained mean, maximum, minimum, standard deviation, and error are shown in Table 2. The error is the difference between the estimated volume and the theoretical volume.

V. Adaptative MPC for Gel Dispensing Control

Even though the previous modeling and control approaches [21] achieved good results in their specific cases, they are mostly linear controllers and not suitable when the properties of the gel to be dispensed vary with time and the time delay is significant in the dispensing processes. Linear controllers such as P and PI controllers work well for linear time-invariant (LTI) systems, and PI controllers can also correct the steady-state error. However, linear controllers such as P and PI controllers are not designed to handle significant time-varying properties or significant time delays of the processes [28]. Here we adopt adaptive MPC controllers with a time-varying prediction model that can be adjusted at run time. The fundamental benefit of model predictive control is that it allows us to optimize the present timestep while taking future timesteps into account. This is accomplished by optimizing a finite time horizon while just implementing the current timestep and then optimizing again, repeatedly [29]. When used with online parameter estimation schemes, adaptive MPC becomes a powerful control solution, which is well suited to optimal control of gel dispensing.

Table 2: The obtained mean, maximum, minimum, the standard deviation and the error using a ruby ball (volume= 14.1372 mm^3)

Mean (mm^3)	Max (mm^3)	Min (mm^3)	Std (mm^3)	Error (mm^3)
14.1982	14.1999	14.1970	5.50×10^{-4}	0.0610

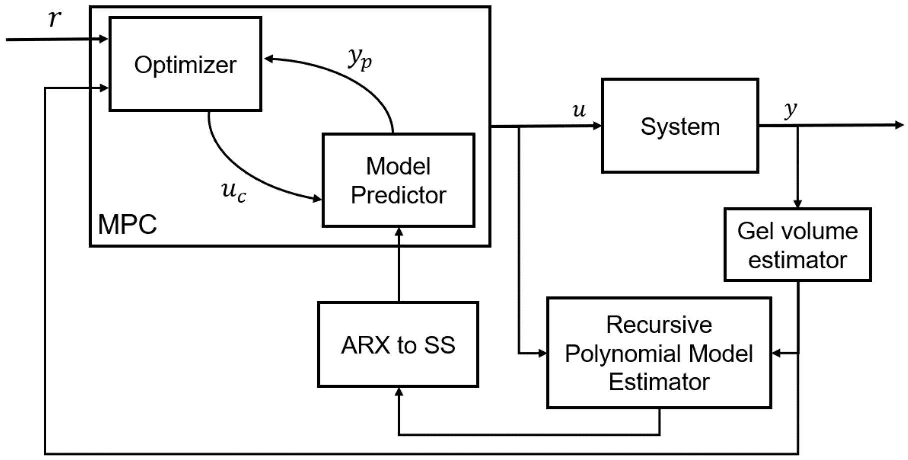

Fig. 6. Adaptative MPC for gel extrusion volume control.

To implement the adaptive MPC, we first create an initial model predictive controller for the nominal operating conditions of the system based on the ARX model (see **Fig. 6**), then update the plant model and nominal conditions used by the MPC controller iteratively at runtime using the method similar to [30] [31].

The prediction model for our adaptive MPC is a linear time-varying, discrete-time state-space model:

$$\begin{aligned} x(k+1) &= Ax(k) + Bu(k) \\ y(k) &= Cx(k) + Du(k) \end{aligned} \tag{2}$$

where the matrices A, B, C, and D are a function of time, k is the time index; x is the model states; u is the plant inputs, in our case the position of the pusher that can be adjusted by the MPC controller; y is the plant output, which is the gel volume.

The gel volume $y(k)$ should follow as closely as possible the varying setpoint or reference $r(k)$ of the desired volume. To establish the control law, we should find a suitable $u(k)$ solution that minimizes the cost function J [32]:

$$J = \sum_{i=1}^{N_p} Q\big(r(k+i) - \hat{y}(k+i)\big)^2 + \sum_{i=1}^{N_c} w\big(\Delta u(k+i-1)\big)^2$$
$$s.t.\, lb \le \Delta u \le ub \tag{3}$$

where Q and w are the weights, $\hat{y}$ is the estimated gel volume by machine vision algorithm in Section III, Δu is the incremental control input of the current time step compared to the previous step, N_p is the prediction horizon, N_c is the control horizon, both are in time steps.

The set of allowable values for the incremental input Δu is bounded by both upper and lower saturation limits in the pusher tip of the dispenser lb and ub, to avoid overflowing the gel from the dispenser and the system goes out of the controllable space where the pusher will mechanically malfunction.

At each time step, a new constrained optimization problem of Eq. (3) is solved, obtaining in a series of N_c control horizon, or future moves that minimize the cost function based on the inputs at the past and current time steps. This is achieved by iteratively searching best solutions using a model predictor of Eq (2), where the optimizer evaluates the estimated output volume y_c from the model predictor by exploring u_c in the search space (see **Fig. 6**). The horizon is shifted forward one sampling time at the next time step, and the optimization is repeated. Because the horizons are constantly shifting, they are often referred to as receding horizons.

Eq. (3) optimizes a quantity that is divided into two parts. The first part expresses the expected error between future model predictions $\hat{y}$ and the future setpoints r. Increasing the weight Q penalizes the expected error proportionally, which makes the error reduces faster. The second part of Eq. (3) quantifies the change in control moves. Increasing the weight w, penalizes the change in control moves, which discourages the controller from making dramatic actuation. A careful selection of these two weights Q and w is important to achieve successful volume control.

A discrete-time auto-regressive with exogenous input (ARX) model is identified online by the Recursive Polynomial Model Estimator block (see **Fig. 6**) at each time step. The adaptive MPC controller uses the model to update the internal plant model to control the time-variant gel dispensing process. The ARX model [32],

$$AA(k-1)y(k) = BB(k-1)u(k) \tag{4}$$

can be arranged to give the current output in terms of the past outputs and current and past inputs as [32],

$$y(k) = -a_1 y(k-1) \cdots - a_n y(k-n) + b_0 u(k) + b_1 u(k-1) + \cdots + b_m u(k-m) \tag{5}$$

We need to estimate the $n+m+1$ unknown parameters a_1, $\ldots, a_n$ and b_0, …, b_m such that our model is a reasonable approximation to the data collected from the gel dispenser. Notice that based on preliminary experimental identification of the system, the order n is chosen to be 2, where $n \ge m$. We can collect all unknown parameters into a column vector, θ, defined as

$$\theta = [\, a_1\, a_2 \cdots a_n \mid b_0\, b_1 \cdots b_m]^T \tag{6}$$

and the immediate past data vector as

$$\varphi^T = [-y(k-1)\ -y(k-2)\cdots -y(k-n)\ \ u(k)\ u(k-1)\cdots\ u(k-m)] \qquad (7)$$

The Recursive Polynomial Model Estimator in **Fig. 6** estimates an ARX model from the displacement of the pusher tip (input) and the measured gel volume (output). The estimated model is then converted into state-space form and fed to the Adaptive MPC Controller at each time step.

To avoid slow convergence of the estimated parameters of the model due to continuous parameters variation, a forgetting

Algorithm 1: Online recursive polynomial model estimation algorithm.

1. At time step N, collect a new input/output data pair (u_{N+1}/y_{N+1});
2. Form the new φ_{N+1} vector by inserting u_{N+1}, y_{N+1} into:

$$\varphi_{N+1}^T = [-y_N\ \dots - y_{N-n+1} |\ u_{N+1}\ \dots\ u_{N-m+1}] \qquad (8)$$

3. Evaluate the new gain matrix K_{N+1} [23]

$$K_{N+1} = \frac{P_N \varphi_{N+1}}{\lambda + \varphi_{N+1}^T P_N \varphi_{N+1}} \qquad (9)$$

where the covariance matrix $P_N = (X_N^T X_N)^{-1}$ and λ is the forgetting factor.

X_N is the old data matrix,

$$X_N = \left[\begin{array}{cccc|cccc} -y_{n-1} & -y_{n-2} & \cdots & -y_0 & u_n & u_{n-1} & \cdots & u_{n-m} \\ -y_n & -y_{n-1} & \cdots & -y_1 & u_{n+1} & u_n & \cdots & u_{n-m+1} \\ \vdots & \vdots & \ddots & \vdots & \vdots & \vdots & \ddots & \vdots \\ -y_{N-1} & -y_{N-2} & \cdots & -y_{N-n-1} & u_N & u_{N-1} & \cdots & u_{N-m} \end{array}\right] \qquad (10)$$

4. Update the parameter vector θ_{N+1} [23]

$$\theta_{N+1} = \theta_N + K_{N+1}(y_{N+1} - \varphi_{N+1}^T \theta_N) \qquad (11)$$

5. Update the covariance matrix P_{N+1}, which is required for the next iteration [23].

$$P_{N+1} = \frac{P_N}{\lambda}[\mathrm{I} - \varphi_{N+1} K_{N+1}^T] \qquad (12)$$

6. Wait out the remainder of one sample time T, increase the sample counter, N to $N+1$, then go back to step 1.

factor is used to gradually reduce the influence of old data in favor of more recent data. The initial model is obtained using offline system identification, which is used to initialize the online estimator. The algorithm of the online recursive polynomial model estimator is described step-by-step in Algorithm 1.

The whole scheme of visual servoing adaptive MPC for gel dispensing control is shown in **Fig. 6**. The controller performance is validated experimentally at a sampling frequency of 20 Hz. The Recursive Polynomial Model Estimator above is used to estimate an ARX model based on the displacement of the dispenser tip (input) and the measured gel volume (output). The weights of the cost function Q and w have been selected based on the trial-error method ($Q = 5.2, w = 0.8$). A 0.98 forgetting factor has been selected based on trial-and-error. The adaptive MPC scheme was evaluated using the experimental setup

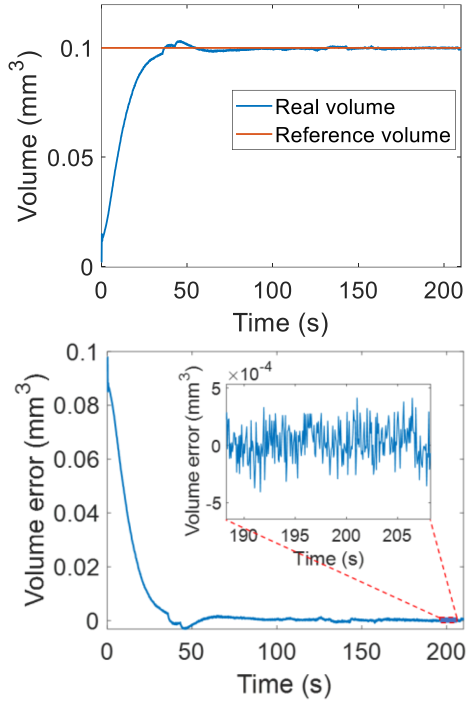

Fig. 7. Dispensed gel volume controlled by the adaptive MPC, compared with the reference volume, as well as the corresponding volume error.

presented in section II. As shown in **Fig. 7,** for a reference volume of 0.1 mm^3 at $t = 0\,s$, the real volume tracks the reference volume with a response time of 55 s, and a volume tracking error of $2.44 \times 10^{-4} mm^3$ (0.24%). The response time is very important to avoid the overflow of the extruded gel and consequently control failure. For this reason, we designed the controller to be slow at the beginning to avoid overflow.

VI. FIBER THREADING USING ROBOTIC GEL DISPENSING

In this section, we investigate the impact of the proposed gel dispensing volume control method when combined with the fiber threading method on the repeatability of the mechanical properties of the fabricated fibers, where the whole approach is abbreviated as IMPVC in short. We use an experimental protocol as shown in **Fig. 1** to conduct experiments and characterize the mechanical properties of the fabricated fibers and investigate the repeatability of the experiments.

To investigate the repeatability of the mechanical properties of the proposed IMPVC method, four fibers are fabricated and characterized following the experimental protocol of **Fig. 1**. The dispensed gel volume is 0.6 mm^3 in all experiments. The obtained characterization force-extension curves are shown in **Fig. 8 (a)**. The mean, standard deviation (SD), and coefficient of variation (CV) of the mechanical properties, toughness, stiffness, elongation, and strength are estimated as shown in Table 3.

To compare the results, we also studied the repeatability of the mechanical properties using the VRVC method. A dispensed volume of 0.6 mm^3 in VRVC method is used. The obtained characterization force-extension curves for the VRVC method are shown in **Fig. 8 (b)** and the obtained mechanical properties are shown in Table 4. The CV diagram of mechanical properties

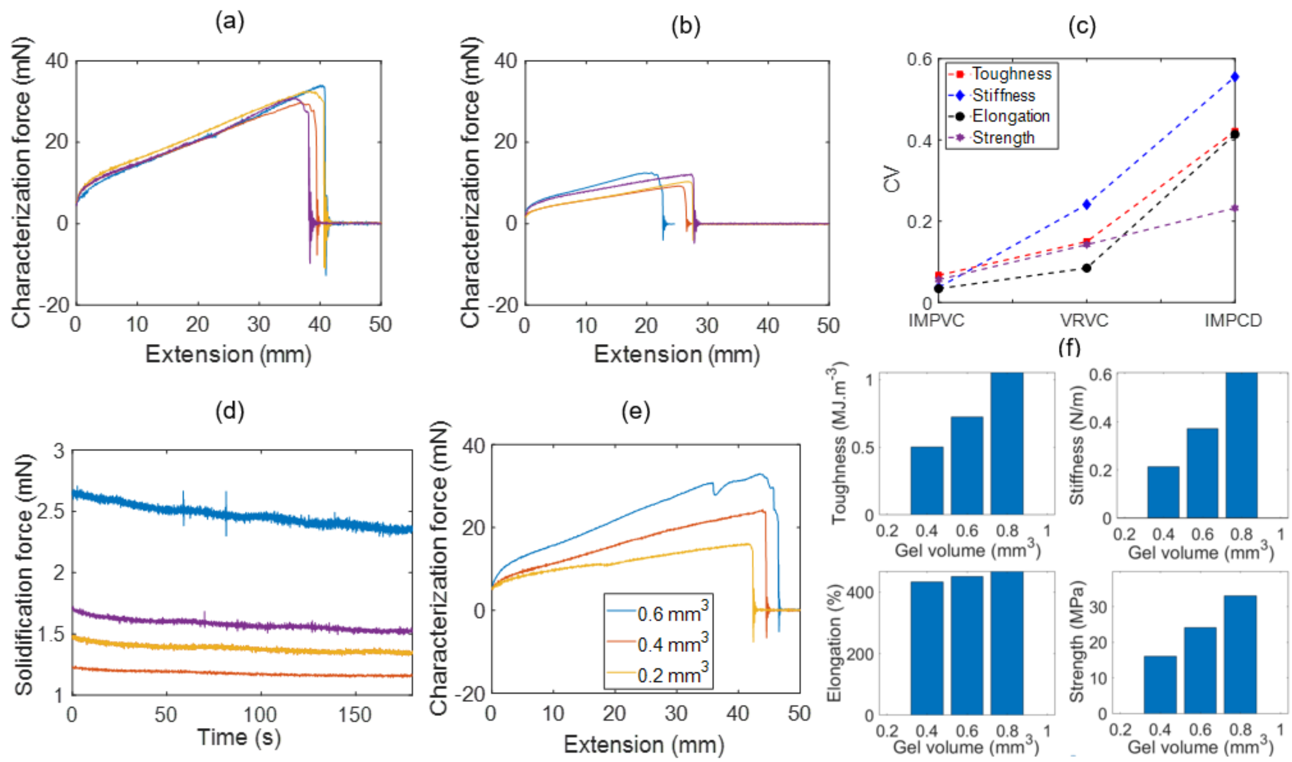

Fig. 8. Force-extension curves during characterization for a) IMPVC method; b) VRVC method. c) The obtained CV of toughness, stiffness, elongation, and strength for IMPVC, VRVC, and IMPCD. d) The pulling force during solidification using VRVC method with volumes of 0.6 mm^3. e) Characterization of three fibers using IMPVC with the volumes of 0.2, 0.4, and 0.6 mm^3. f) The obtained mechanical properties: toughness, stiffness, elongation, and strength, for fiber threading using IMPVC with volumes of 0.2, 0.4, and 0.6 mm^3.

(toughness, stiffness, elongation, and strength) is shown in **Fig. 8 (c)**.

We can notice that the repeatability of the mechanical properties using the IMPVC method is the highest (with the lowest CV in **Fig. 8 (c)** and using the VRVC method ranks second. We attribute the inferior repeatability of the VRVC method to the uncontrolled solidification forces during the fabrication phase as shown in **Fig. 8 (d),** compared with the impedance-controlled solidification in the IMPVC method. On the other hand, the IMPCD method has the lowest repeatability of mechanical properties. We attribute this to the poor volume consistency even though the dispenser parameters are the same, where the mean and SD of 30 repetitions of dispensing are 0.53 and 0.19 mm^3 respectively. The results also show that the initial volume has a significant impact on the mechanical properties of the fabricated fibers.

TABLE 3: TOUGHNESS, STIFFNESS, ELONGATION, AND STRENGTH, FOR FIBER FABRICATED BASED ON IMPEDANCE CONTROL WITH VOLUME CONTROL

	Toughness ($MJ \cdot m^{-3}$)	Stiffness (N/m)	Elongation (%)	Strength (MPa)
Mean	0.82	0.62	401.2	31.79
SD	0.06	0.023	13.7	1.79
CV (%)	7.32	3.71	3.41	5.63

TABLE 4: TOUGHNESS, STIFFNESS, ELONGATION, AND STRENGTH, FOR FIBER FABRICATED BASED ON VELOCITY REGULATION WITH VOLUME CONTROL

	Toughness ($MJ \cdot m^{-3}$)	Stiffness (N/m)	Elongation (%)	Strength (MPa)
Mean	0.20	0.29	176.0	11.09
SD	0.03	0.070	14.9	1.58
CV (%)	15.00	24.14	8.48	14.25

To study the influence of the initial volume on the mechanical properties of the fabricated fibers using the proposed IMPVC method, we extruded different volumes of 0.2, 0.4, and 0.6 mm^3. The obtained force-extension curves are shown in **Fig. 8 (e)**. The mechanical properties of the fabricated fibers, in terms of toughness, stiffness, elongation, and strength corresponding to a different volume, are compared using bar diagrams as shown in **Fig. 8 (f).** We can notice that the toughness, stiffness, elongation, and strength are directly proportional to the extruded gel volume, in line with the expectation.

VII. CONCLUSION

Fluid dispensing is widely used in a variety of sectors, including industrial applications such as garment and footwear manufacturing and assembly, soft macro-, and microrobotics. In this paper, we proposed an online precise robotic gel dispensing method to achieve highly repeatable robotic fiber fabrication.

We designed a robotic gel dispenser that can accurately dispense gel droplets of desired volume using visual servoing and adaptive model predictive control. An online 3-dimensional gel volume estimation algorithm based on image processing was constructed to provide the estimation of the volume of the dispensed gel droplet during dispensing. We employ the fiber threading technique based on impedance control with force tracking we developed recently to carry out the fiber threading experiments. To examine the benefits of the accuracy of the dispensed droplet, multiple fiber threading experiments were conducted, where the repeatability of the fibers fabricated using the proposed methods was compared with two other methods: a) conventionally velocity regulation-based fiber fabrication, where the pulling force profile is not controlled, and b) fiber threading using impedance control with force tracking using a commercial time-pressure dispenser. The obtained gel volume estimation standard deviation is $5.50 \times 10^{-4}\ mm^3$, with extruded gel volume tracking error of $2.43\times 10^{-4} mm^3$ (0.24%). The proposed approach in the paper gave the best repeatability. The obtained CV of the toughness, stiffness, elongation, and strength is 6.7%, 3.7%, 3.4%, and 5.6% respectively. The influence of the extruded gel volume has been studied, showing that the mechanical properties of toughness, stiffness, elongation, and strength are directly proportional to the increase of the extruded gel volume.

Acknowledgment

This work has been supported by the project 317018 AI spider silk threading (ASSET) in the AIPSE program of the Academy of Finland.

References

[1] D. Ye, Y. Ding, Y. Duan, J. Su, Z. Yin, and Y. A. Huang, "Large-Scale Direct-Writing of Aligned Nanofibers for Flexible Electronics," *Small*, vol. 14, no. 21, p. 1703521, May 2018, doi: 10.1002/SMLL.201703521.

[2] C. F. Guimarães, L. Gasperini, A. P. Marques, and R. L. Reis, "3D flow-focusing microfluidic biofabrication: One-chip-fits-all hydrogel fiber architectures," *Appl Mater Today*, vol. 23, p. 101013, Jun. 2021, doi: 10.1016/J.APMT.2021.101013.

[3] H. Bettahar, C. Clévy, F. Behague, N. Courjal, and P. Lutz, "Novel Strategy for High Precision Automated Robotic Positioning based on Fabry-Perot Interferometry Principle," *IEEE International Conference on Automation Science and Engineering*, vol. 2018-August, pp. 1441–1447, Dec. 2018, doi: 10.1109/COASE.2018.8560700.

[4] H. Bettahar, C. Clevy, N. Courjal, and P. Lutz, "Force-Position Photo-Robotic Approach for the High-Accurate Micro-Assembly of Photonic Devices," *IEEE Robot Autom Lett*, vol. 5, no. 4, pp. 6396–6402, Oct. 2020, doi: 10.1109/LRA.2020.3014634.

[5] H. Bettahar, O. Lehmann, C. Clevy, N. Courjal, and P. Lutz, "6-DoF Full Robotic Calibration Based on 1-D Interferometric Measurements for Microscale and Nanoscale Applications," *IEEE Transactions on Automation Science and Engineering*, vol. 19, no. 1, pp. 348–359, Jan. 2022, doi: 10.1109/TASE.2020.3031856.

[6] H. Bettahar, "High accurate 3-D photo-robotic nano-positioning for hybrid integrated optics," Jul. 2019, Accessed: Mar. 27, 2023. [Online]. Available: https://theses.hal.science/tel-02363255

[7] W. Eom *et al.*, "Large-scale wet-spinning of highly electroconductive MXene fibers," *Nature Communications 2020 11:1*, vol. 11, no. 1, pp. 1–7, Jun. 2020, doi: 10.1038/s41467-020-16671-1.

[8] Z. Yang *et al.*, "On the cross-section of shaped fibers in the dry spinning process: Physical explanation by the geometric potential theory," *Results Phys*, vol. 14, p. 102347, Sep. 2019, doi: 10.1016/J.RINP.2019.102347.

[9] J. Xue, T. Wu, Y. Dai, and Y. Xia, "Electrospinning and electrospun nanofibers: Methods, materials, and applications," *Chemical Reviews*, vol. 119, no. 8. NIH Public Access, pp. 5298–5415, Apr. 24, 2019. doi: 10.1021/acs.chemrev.8b00593.

[10] X. Wu *et al.*, "Microfluidic-spinning construction of black-phosphorus-hybrid microfibres for non-woven fabrics toward a high energy density flexible supercapacitor," *Nature Communications 2018 9:1*, vol. 9, no. 1, pp. 1–11, Nov. 2018, doi: 10.1038/s41467-018-06914-7.

[11] D. Ye *et al.*, "Large-Scale Direct-Writing of Aligned Nanofibers for Flexible Electronics," *Wiley Online Library*, vol. 14, no. 21, May 2018, doi: 10.1002/smll.201703521.

[12] M. Andersson *et al.*, "Biomimetic spinning of artificial spider silk from a chimeric minispidroin," *Nature Chemical Biology 2017 13:3*, vol. 13, no. 3, pp. 262–264, Jan. 2017, doi: 10.1038/nchembio.2269.

[13] X. Zhang *et al.*, "CRISPR/Cas9 Initiated Transgenic Silkworms as a Natural Spinner of Spider Silk," *Biomacromolecules*, vol. 20, no. 6, pp. 2252–2264, Jun. 2019, doi: 10.1021/ACS.BIOMAC.9B00193.

[14] C. Belbéoch, J. Lejeune, P. Vroman, and F. Salaün, "Silkworm and spider silk electrospinning: a review," *Environmental Chemistry Letters 2021 19:2*, vol. 19, no. 2, pp. 1737–1763, Jan. 2021, doi: 10.1007/S10311-020-01147-X.

[15] H. Bettahar, P. A. D. Harischandra, and Q. Zhou, "Robotic Threading from a Gel-like Substance Based on Impedance Control with Force Tracking," *IEEE Robot Autom Lett*, vol. 7, no. 1, pp. 33–40, Jan. 2022, doi: 10.1109/LRA.2021.3116697.

[16] H. Bettahar, T. Valisalmi, M. Linder, and Q. Zhou, "Robotic Fiber Fabrication based on Solidification Force Control," *Proceedings of MARSS 2022 - 5th International Conference on Manipulation, Automation, and Robotics at Small Scales*, 2022, doi: 10.1109/MARSS55884.2022.9870490.

[17] X. Chen, J. K.-I. transactions on electronics packaging, and undefined 2004, "Modeling of positive-displacement fluid dispensing processes," *ieeexplore.ieee.org*. Available: https://ieeexplore.ieee.org/abstract/document/1393071/

[18] Y. Zhao, X. C.-T. I. J. of A. Manufacturing, and undefined 2011, "Model-based robust design for time–pressure fluid dispensing using surrogate modeling," *Springer*, vol. 55, no. 5–8, pp. 433–446, Jul. 2011, doi: 10.1007/s00170-010-3108-2.

[19] C. Zhou, J. A. Duan, G. Deng, and J. Li, "A Novel High-Speed Jet Dispenser Driven by Double Piezoelectric Stacks," *IEEE Transactions on Industrial Electronics*, vol. 64, no. 1, pp. 412–419, Jan. 2017, doi: 10.1109/TIE.2016.2598805.

[20] S. Z. Liu, J. Y. Peng, Y. B. Zhang, and X. B. Chen, "Modeling rotary-screw-driven dispensing systems for electronics packaging," *IEEE Trans Compon Packaging Manuf Technol*, vol. 4, no. 8, pp. 1359–1365, 2014, doi: 10.1109/TCPMT.2014.2325894.

[21] M. Reighard, J. Byers, … R. Z.-U. P., and undefined 2001, "Viscous material dispensing system and method with feedback control," *Google Patents*, 2001, Accessed: Jun. 15,

2022. [Online]. Available: https://patents.google.com/patent/US6173864B1/en
[22] X. B. Chen, W. J. Zhang, G. Schoenau, and B. Surgenor, “Off-line control of time-pressure dispensing processes for electronics packaging,” *IEEE Transactions on Electronics Packaging Manufacturing*, vol. 26, no. 4, pp. 286–293, Oct. 2003, doi: 10.1109/TEPM.2003.820824.
[23] H. Li, J. Liu, C. Chen, H. D.-I. T. on, and undefined 2007, “A simple model-based approach for fluid dispensing analysis and control,” *ieeexplore.ieee.org*, vol. 12, no. 4, 2007, doi: 10.1109/TMECH.2007.901946.
[24] S. Liu, D. Xu, Y. Li, … F. S.-I. T. on, and undefined 2016, “Nanoliter fluid dispensing based on microscopic vision and laser range sensor,” *ieeexplore.ieee.org*, Accessed: Jun. 15, 2022. [Online]. Available: https://ieeexplore.ieee.org/abstract/document/7572188/
[25] Y. X. Zhao and X. Du Chen, “Model-based robust design for time–pressure fluid dispensing using surrogate modeling,” *The International Journal of Advanced Manufacturing Technology 2010 55:5*, vol. 55, no. 5, pp. 433–446, Dec. 2010, doi: 10.1007/S00170-010-3108-2.
[26] K. Thurow, T. Krüger, and N. Stoll, “An optical approach for the determination of droplet volumes in nanodispensing,” *J Autom Methods Manag Chem*, vol. 2009, 2009, doi: 10.1155/2009/198732.
[27] S. Boonsang and W. Lertkittiwattanakul, “A flash photography method for the measurements of the fluid flow dynamic of a fluid dispensing system,” *Measurement (Lond)*, vol. 102, pp. 57–63, May 2017, doi: 10.1016/j.measurement.2017.01.050.
[28] X. B. Chen, “Modeling and control of fluid dispensing processes: a state-of-the-art review”, doi: 10.1007/s00170-008-1700-5.
[29] A. Afram and F. Janabi-Sharifi, “Theory and applications of HVAC control systems – A review of model predictive control (MPC),” *Build Environ*, vol. 72, pp. 343–355, Feb. 2014, doi: 10.1016/J.BUILDENV.2013.11.016.
[30] V. Adetola and M. Guay, “Robust adaptive MPC for constrained uncertain nonlinear systems,” *Int J Adapt Control Signal Process*, vol. 25, no. 2, pp. 155–167, Feb. 2011, doi: 10.1002/ACS.1193.
[31] X. Wang, K. Ma, and Y. Wang, “Adaptive power control with online model estimation for chip multiprocessors,” *IEEE Transactions on Parallel and Distributed Systems*, vol. 22, no. 10, pp. 1681–1696, 2011, doi: 10.1109/TPDS.2011.39.
[32] “Model Predictive Control System Design and Implementation Using MATLAB® - Liuping Wang - Google Books.”